

# Improved Track Reconstruction Performance for Long-lived Particles in ATLAS

JACKSON BURZYNSKI

*On behalf of the ATLAS Collaboration  
Department of Physics  
Simon Fraser University, Burnaby BC, Canada*

## ABSTRACT

Searches for long-lived particles (LLPs) are among the most promising avenues for discovering physics beyond the Standard Model at the LHC. However, displaced signatures are notoriously difficult to identify due to their ability to evade standard object reconstruction strategies. In particular, the default ATLAS track reconstruction applies strict pointing requirements which limit sensitivity to charged particles originating far from the primary interaction point. To recover efficiency for LLPs decaying within the tracking detector volume, ATLAS employs a dedicated large-radius tracking (LRT) pass with loosened pointing requirements, taking as input the hits left over from the primary track reconstruction. During Run 2 of the LHC, the LRT implementation was highly efficient but suffered from a large number of incorrectly reconstructed track candidates which prohibited it from being run in the standard reconstruction chain. Instead, a small subset of the data was preselected for LRT reconstruction using information from the standard object reconstruction. In preparation for LHC Run 3, ATLAS has completed a major effort to improve both standard and large-radius track reconstruction performance which allows for LRT to run in all events, expanding the potential phase-space of LLP searches and streamlining their analysis workflow. These proceedings summarize these achievements and report on the readiness of the ATLAS detector for track-based LLP searches in Run 3.

## PRESENTED AT

Connecting the Dots Workshop (CTD 2022)  
May 31 - June 2, 2022

# 1 Introduction

In order to reconstruct the trajectories of charged particles (tracks), ATLAS [1] uses the Inner Detector (ID) tracking system to provide efficient, robust and precise position measurements of charged particles as they traverse the detector. The ID is immersed in a 2 T axial magnetic field and is comprised of three subdetectors. The high-granularity silicon pixel detector consists of concentric barrel layers with  $r = 33, 50.5, 88.5, \text{ and } 122.5 \text{ mm}^1$  in the central region, and three disks in each of the endcaps at  $|z| = 495, 580, \text{ and } 650 \text{ mm}$ . The pixel detector is followed by the silicon microstrip tracker (SCT), consisting of barrel layers at  $r = 299, 371, 443, \text{ and } 514 \text{ mm}$  and nine wheels in each of the endcaps with  $854 < |z| < 2720 \text{ mm}$ . These silicon detectors are complemented by the transition radiation tracker (TRT) composed of straw tubes which run parallel to the beamline in the barrel, enabling radially extended track reconstruction up to  $|\eta| = 2.0$ .

Tracks are reconstructed from the energy deposits (hits) recorded in individual detector elements of the ID. The standard ATLAS track reconstruction algorithm is optimized for reconstructing tracks that originate in the vicinity of the primary interaction point (IP), and is not efficient for reconstructing tracks that are displaced by more than 5 mm from the IP due to tight selections placed on the transverse and longitudinal impact parameters. Thus, to reconstruct displaced tracks originating from the decays of long-lived particles (LLPs), a secondary *large-radius tracking* (LRT) algorithm [2] is used which improves the ATLAS track reconstruction efficiency for a larger particle lifetime range.

In preparation for the LHC Run 3 data-taking, the LRT algorithm has undergone a substantial reoptimization. An overview of the LRT algorithm and the improvements with respect to the Run 2 implementation is given in Section 2. The performance of the updated LRT configuration is then evaluated on simulated samples of benchmark long-lived particle scenarios in Section 3, and comparisons are performed between data and simulated inelastic proton-proton collisions in Section 4.

## 2 Large-radius tracking

The LRT reconstruction is performed after the standard ATLAS track reconstruction, taking as input the hits that are unassociated to standard tracks. It follows the same reconstruction strategy as the standard tracking but with modified selections that are tuned to achieve improved performance for reconstructing displaced particles, most notably on the maximally allowed values of the transverse and longitudinal impact parameters ( $d_0$  and  $z_0$ ). By relaxing the selections on  $|d_0|$  and  $|z_0|$  to 300 mm and 500 mm, respectively, the LRT algorithm is able to reconstruct charged particles with efficiencies greater than 75% for production radii ( $r_{\text{prod}}$ ) of 300 mm or less.

For the LHC Run 2 data-taking period (2015-2018) the LRT algorithm was predominantly optimized for high signal efficiency, resulting in approximately twice the computational time per event compared to the prompt pass due to a very high rate of poor-quality tracks, including “fake” tracks reconstructed from random hit combinations and tracks from soft material interactions [2]. This increased processing time was affordable because the LRT reconstruction was only applied to an  $\mathcal{O}(10\%)$  fraction of the events recorded by the ATLAS detector that were selected based on event-level quantities computed during the standard reconstruction. For the LHC Run 3 (2022-2024) data-taking, the average number of simultaneous  $pp$  collisions per bunch crossing ( $\langle\mu\rangle$ ) is expected to increase to 50 from Run 2 values that ranged between 20 and 40. In preparation for these challenging Run 3 conditions, the LRT pass has been updated, significantly reducing the computation time for track reconstruction for LLP signatures while reducing the rate of fake tracks by roughly 95%. As a consequence of these improvements, a full integration of the LRT reconstruction for LLP signatures into the standard ATLAS event reconstruction chain was achieved (see [3] for details on the Run 3 tracking software performance).

---

<sup>1</sup>ATLAS uses a right-handed coordinate system with its origin at the nominal interaction point (IP) in the centre of the detector and the  $z$ -axis along the beam pipe. The  $x$ -axis points from the IP to the centre of the LHC ring, and the  $y$ -axis points upward. Cylindrical coordinates  $(r, \phi)$  are used in the transverse plane,  $\phi$  being the azimuthal angle around the beam pipe. The pseudorapidity is defined in terms of the polar angle  $\theta$  as  $\eta = -\ln[\tan(\theta/2)]$ .

### 3 Performance studies on simulation

Two benchmark signal models are used to assess the displaced track reconstruction efficiency targeting leptonic and hadronic secondary vertex signatures. The first is a displaced heavy-neutral-lepton (HNL) signal, which results in a characteristic dilepton displaced vertex. The HNL signal mass is 15 GeV and the proper lifetime  $c\tau$  is 100 mm. The second is a simplified model in which a new electrically neutral pseudoscalar boson  $a$  is produced in pairs through decays of the Higgs boson, with the  $a$  boson subsequently decaying into pairs of  $b$ -quarks. This LLP decay results in a hadronic displaced vertex signature which tends to have higher track multiplicity than the HNL signature. The  $a$  boson mass is 55 GeV and the proper lifetime  $c\tau$  is 100 mm. Detailed signal descriptions of the two models can be found in Refs [4] and [5].

To assess the reconstruction efficiency in simulation, a hit-based matching scheme is used to associate reconstructed tracks to truth-level particles. The track reconstruction efficiency is then defined as the ratio of the number of signal truth particles matched to reconstructed tracks divided by the number of signal truth particles. Truth particles are subject to the fiducial selections shown in Table 1. The resulting efficiency is referred to as the “technical” efficiency, and quantifies the reconstruction performance for truth particles that are expected to satisfy the necessary requirements to be reconstructed by the tracking algorithm. The track reconstruction efficiencies for the two benchmark models are shown in Figure 1 as a function of  $|d_0|$  for standard tracking, LRT, and the combined collection of standard and large-radius tracks. After  $|d_0| > 5$  mm, the standard track reconstruction efficiency becomes negligible with LRT recovering the loss in efficiency with significant efficiencies out to  $|d_0| = 300$  mm. The observed efficiencies are on the order of 10% smaller than those obtained with the Run 2 LRT configuration. This is due to an overall tightening of the track selections imposed to reduce the number of fake tracks reconstructed and improve the computational performance.

Table 1: Fiducial selections applied to truth particles entering into the technical efficiency calculation.

$p_T > 1$ GeV
$ \eta  < 2.5$
$r_{\text{prod}} < 440$ mm
charge = $\pm 1$
$N_{\text{hits}}^{\text{Si}} > 8$
From LLP decay

#### 3.1 Impact on searches for displaced vertices

Many analyses which used LRT in Run 2 attempted to reconstruct the decays of long-lived particles by performing an additional secondary vertex reconstruction using both standard and LRT tracks. Thus, to evaluate the impact of the improved Run 3 LRT configuration at the analysis level it is most useful to study how the updated track reconstruction changes the LLP vertex reconstruction efficiency and the overall rate of vertices reconstructed from fake tracks, which correspond to the dominant backgrounds in such searches.

The study is performed using the benchmark model of a displaced hadronic decay described in Section 3. To compare the performance between Run 2 and Run 3, the simulated events are reconstructed using the Run 2 and Run 3 ATLAS track reconstruction configurations. Secondary vertices are reconstructed using a dedicated inclusive vertexing algorithm optimized for identifying the decays of heavy long-lived particles [7]. Identical vertex reconstruction configurations are used for the two samples.

To assess the signal vertex reconstruction efficiency and evaluate the impact of fake tracks, a truth-matching procedure is performed. Reconstructed vertices are considered matched to an LLP decay if the  $p_T$ -weighted fraction of tracks in the vertex that are matched to truth-level LLP descendants is greater than 0.5. Figure 2 shows the radial distributions of truth-matched and non-truth-matched vertices for the Run 2 and Run 3 samples. The Run 3 reconstruction has a modest increase in the number of LLP vertices and considerably fewer non-LLP vertices due to the significant increase in purity of the LRT algorithm.

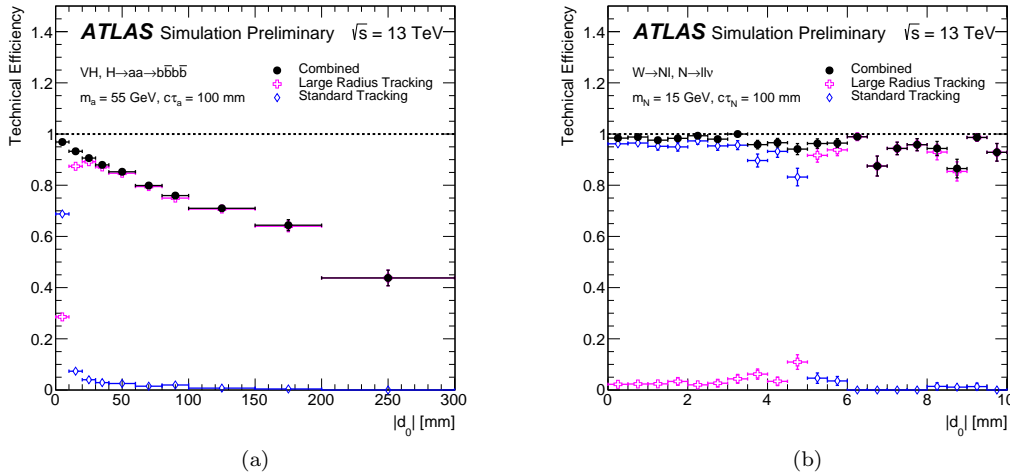


Figure 1: The technical track reconstruction efficiency for displaced charged particles produced by the decay of (a) long-lived scalar particles decaying hadronically, and (b) long-lived heavy neutral leptons decaying leptonically. The efficiency is shown as a function of the absolute value of the transverse impact parameter,  $|d_0|$ . The efficiencies are computed using standard tracks only (blue), large-radius tracks only (pink), as well as the combined collection of standard and large-radius tracks (black) [6].

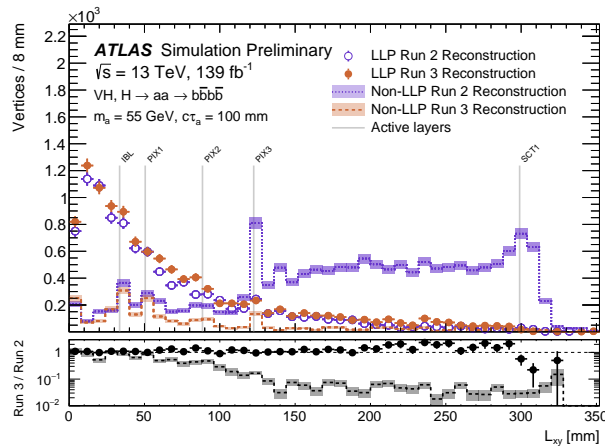


Figure 2: A comparison of the radial distributions of reconstructed secondary vertices in a simulated long-lived particle sample using the Run 2 and Run 3 track reconstruction configurations. The circular markers represent reconstructed vertices that are matched to truth-level LLP decay vertices (LLP). The dashed lines represent reconstructed vertices that are not matched to truth-level LLP decay vertices (non-LLP). The four pixel layers and first SCT layer are shown in the figure with vertical lines [6].

## 4 Data and simulation comparison

To further validate the improved LRT configuration, comparisons are performed between Run 2 data and simulated inelastic proton-proton collisions. Data were selected from the 2018 data taking period using an unbiased random trigger (the ‘zero-bias’ trigger) which fires on the bunch crossing occurring one LHC revolution after a low-threshold calorimeter-based trigger. This trigger runs throughout the normal ATLAS data-taking, ensuring that the data is obtained with equivalent beam conditions present in normal physics

data-taking and thus give a representative sample to study the tracking performance. The total number of recorded events is  $25 \times 10^6$  and has  $\langle \mu \rangle = 34$ . The simulation is generated with a flat  $\mu$  profile and is thus reweighted to agree with the  $\mu$  profile of the data. The transverse momentum distributions of tracks were found to be consistent between data and simulation, therefore no additional reweighting is performed. Both data and simulation were reprocessed using the Run 3 reconstruction software [3]. Track-level comparisons are performed (Section 4.1), as well as comparisons of the properties of secondary vertices consistent with the decays of  $K_0^S$  mesons (Section 4.2).

## 4.1 Track properties

The distributions of the number of hits in the pixel and SCT ID subsystems per LRT track are shown in Figure 3. The distributions in the simulation closely match the distributions in data. Small discrepancies are consistent with those observed in the Run 2 LRT configuration [2]. The absolute value of the transverse impact parameter ( $d_0$ ) for reconstructed LRT tracks is shown in Figure 4. The peaks in the distribution at  $|d_0| = 50, 88,$  and  $122$  mm coincide with the radial positions of the three pixel barrel layers, and correspond to low- $p_T$  secondary tracks with trajectories tangential to the material layers. The largest deviations from unity in the ratio of data to simulation are at the 10% level, indicating very good agreement between the two samples.

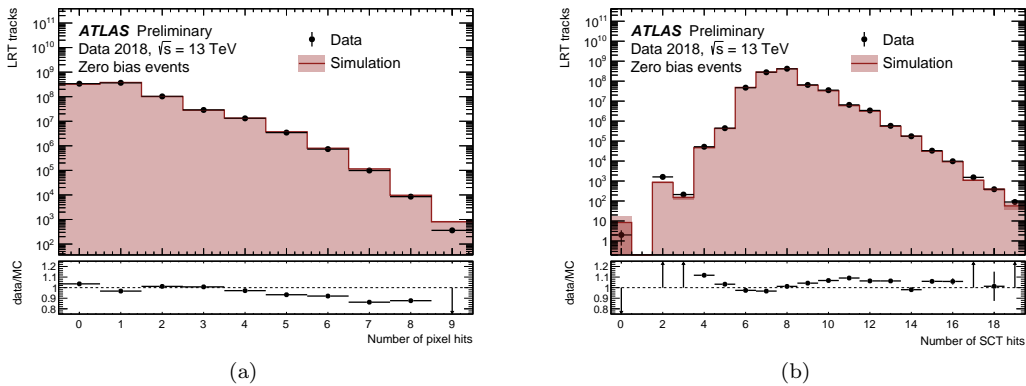


Figure 3: The distribution of the number of hits in the (a) pixel and (b) SCT detector in 2018 zero bias data (black markers) and simulated inelastic proton-proton collisions (filled red histogram). The simulation is normalized to the number of tracks in data. The uncertainty shown in the ratio plot represents the combined statistical uncertainties on the simulation and the data. Points in the ratio that do not lie within the visible range are shown as arrows [8].

## 4.2 Study of $K_0^S$ vertices

To compare the track reconstruction efficiency between data and MC, a “standard candle” is needed to identify LRT tracks originating from a true long-lived particle decay. The  $K_0^S$  meson is an ideal candidate based on its lifetime ( $c\tau = 27$  mm) and clean signature of a two-track vertex. To identify  $K_0^S$  vertices, secondary vertices are reconstructed from the combined collection of standard and large-radius tracks using an algorithm optimized for identifying two-body  $V0$  decays [9].  $K_0^S$  candidates are identified by requiring that the invariant mass of the vertex fit is in the range  $[472, 522]$  MeV. No additional vetoes or background subtractions are applied to the vertex yields. The simulation is normalized to the data based off of the total number of reconstructed  $K_0^S$  candidates.

The radial distribution ( $R_{xy}$ ) of the reconstructed  $K_0^S$  candidates are then compared between data and simulation, as shown in Figure 5a. Vertices in simulation are separated in three categories based on the number of LRT tracks included in the vertex fit. Significant differences in the LRT reconstruction efficiency

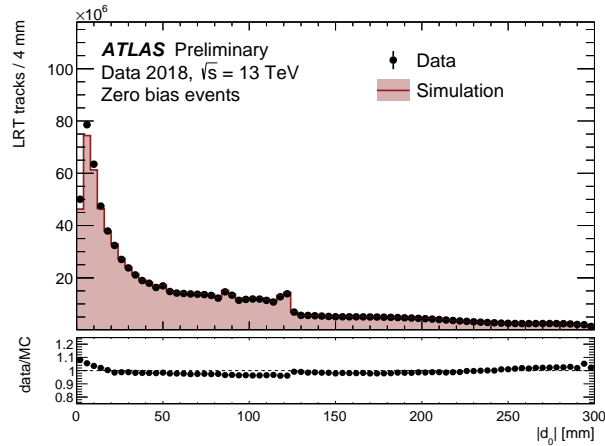


Figure 4: The distribution of the absolute value of the transverse impact parameter ( $d_0$ ) in data (black markers) and simulated inelastic proton-proton collisions (filled red histogram). The simulation is normalized to the number of tracks in data. The uncertainty shown in the ratio plot represents the combined statistical uncertainties on the simulation and the data [8].

between data and MC would manifest as deviations in the distributions at large vertex displacement where vertices with two LRT tracks dominate. No such deviations are observed, indicating good agreement between data and simulation in the LRT reconstruction efficiency. After the first SCT layer, LRT begins to have a diminishing contribution to the total yield because particles produced in this region will traverse insufficient silicon layers to satisfy the LRT hit requirements. Figure 5b shows the fraction of  $K_0^S$  candidate vertices reconstructed with either two standard tracks or with at least one large-radius track in data and simulation. The distributions are consistent between the two samples, further indicating good modeling of the LRT reconstruction in simulation. After  $R_{xy} > 70$  mm, LRT tracks account for more than 50% of the total number of  $K_0^S$  candidate vertices, highlighting the importance of LRT for the reconstruction of displaced vertices.

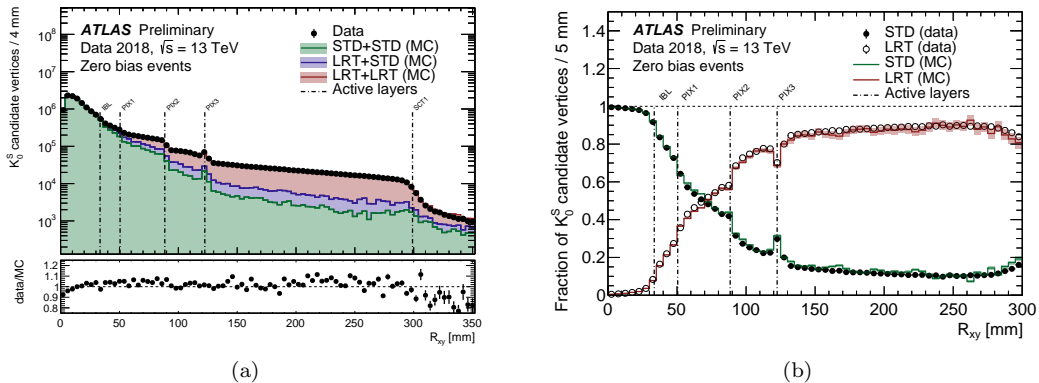


Figure 5: (a) The radial distribution of reconstructed  $K_0^S$  candidate vertices in 2018 zero bias data (black markers) and simulated inelastic proton-proton collisions (stacked histogram). The total number of vertices in simulation is normalized to the number of vertices in data. The four pixel layers and first SCT layer are shown in the figure with dashed vertical lines. (b) The fraction of  $K_0^S$  candidate vertices reconstructed with two standard tracks (labeled “STD” in the legend) and at least one large-radius track (labeled “LRT” in the legend) in 2018 zero bias data (circles) and simulated inelastic proton-proton collisions (histograms) [8].

## 5 Conclusions

The ATLAS large-radius tracking algorithm has undergone significant improvements in preparation for LHC Run 3 data taking. As a result of this reoptimization, a  $\mathcal{O}(95\%)$  reduction in fake tracks was achieved with only a  $\mathcal{O}(10\%)$  reduction in signal track reconstruction efficiency. The large reduction in fakes translates to a drastically reduced CPU time for the track reconstruction, which has allowed for LRT to be integrated in the standard ATLAS reconstruction chain. This will significantly simplify the workflow for LLP analyses in Run 3 as well as allow for analyses not specifically targeting LLP signatures to benefit from increased track reconstruction efficiency at large- $d_0$ . A study of secondary vertex reconstruction for hadronic LLP signatures indicates that the improved LRT configuration leads to a significant reduction in vertices reconstructed from fake tracks and an overall improvement in the vertex reconstruction efficiency for LLP signatures. This will translate directly to improved signal to background ratio for displaced vertex searches in Run 3. Additionally, comparisons between data and simulation show good modeling of both low-level track quantities as well as high-level properties of reconstructed  $K_0^S$  vertices using LRT tracks. These developments are expected to increase the sensitivity of long-lived particle searches in Run 3 and allow for a considerable expansion of the ATLAS LLP search program.

## References

- [1] ATLAS Collaboration, *The ATLAS Experiment at the CERN Large Hadron Collider*, JINST **3** (2008) S08003 (cit. on p. 1).
- [2] ATLAS Collaboration, *Performance of the reconstruction of large impact parameter tracks in the inner detector of ATLAS*, ATL-PHYS-PUB-2017-014, 2017, URL: <https://cds.cern.ch/record/2275635> (cit. on pp. 1, 4).
- [3] ATLAS Collaboration, *Software Performance of the ATLAS Track Reconstruction for LHC Run 3*, tech. rep., CERN, 2021, URL: <https://cds.cern.ch/record/2766886> (cit. on pp. 1, 4).
- [4] ATLAS Collaboration, *Search for heavy neutral leptons in decays of  $W$  bosons using a dilepton displaced vertex in  $\sqrt{s} = 13$  TeV  $pp$  collisions with the ATLAS detector*, (2022), arXiv: 2204.11988 [hep-ex] (cit. on p. 2).
- [5] ATLAS Collaboration, *Search for exotic decays of the Higgs boson into long-lived particles in  $pp$  collisions at  $\sqrt{s} = 13$  TeV using displaced vertices in the ATLAS inner detector*, JHEP **11** (2021) 229, arXiv: 2107.06092 [hep-ex] (cit. on p. 2).
- [6] ATLAS Collaboration, *Expected Large-Radius Tracking Performance in Run 3*, (2021), URL: <https://atlas.web.cern.ch/Atlas/GROUPS/PHYSICS/PLOTS/IDTR-2021-003/> (cit. on p. 3).
- [7] ATLAS Collaboration, *Performance of vertex reconstruction algorithms for detection of new long-lived particle decays within the ATLAS inner detector*, ATL-PHYS-PUB-2019-013, 2019, URL: <https://cds.cern.ch/record/2669425> (cit. on p. 2).
- [8] ATLAS Collaboration, *Run 3 Large-radius tracking performance in data and simulation*, (2022), URL: <https://atlas.web.cern.ch/Atlas/GROUPS/PHYSICS/PLOTS/IDTR-2022-02> (cit. on pp. 4, 5).
- [9] ATLAS Collaboration,  *$K_S^0$  and  $\Lambda$  production in  $pp$  interactions at  $\sqrt{s} = 0.9$  and 7 TeV measured with the ATLAS detector at the LHC*, Phys. Rev. D **85** (2012) 012001, arXiv: 1111.1297 [hep-ex] (cit. on p. 4).